

5-20-2019

## Effects of the Hall Conductivity in Ionospheric Heating Experiments

B. Tulegenov

*Embry Riddle Aeronautical University, TULEGENB@my.erau.edu*

A. V. Streltsov

*Embry-Riddle Aeronautical University, streltsa@erau.edu*

Follow this and additional works at: <https://commons.erau.edu/publication>



Part of the [Atmospheric Sciences Commons](#)

---

### Scholarly Commons Citation

Tulegenov, B., & Streltsov, A. V. (2019). Effects of the Hall conductivity in ionospheric heating experiments. *Geophysical Research Letters*, 46, 6188–6194. <https://doi.org/10.1029/2019GL083340>

This Article is brought to you for free and open access by Scholarly Commons. It has been accepted for inclusion in Publications by an authorized administrator of Scholarly Commons. For more information, please contact [commons@erau.edu](mailto:commons@erau.edu).

# Geophysical Research Letters

## RESEARCH LETTER

10.1029/2019GL083340

### Key Points:

- We investigate effects of Hall conductivity in the ionospheric heating experiments
- The Hall conductivity increases the growth rate and the amplitude of ULF waves generated by the heating
- The Hall conductivity changes the orientation and direction of propagation of the generated waves

### Correspondence to:

B. Tulegenov,  
 tulegenb@my.erau.edu

### Citation:

Tulegenov, B., & Streltsov, A. V. (2019). Effects of the Hall conductivity in ionospheric heating experiments. *Geophysical Research Letters*, *46*, 6188–6194. <https://doi.org/10.1029/2019GL083340>



Received 15 APR 2019

Accepted 21 MAY 2019

Accepted article online 29 MAY 2019

Published online 20 JUN 2019

## Effects of the Hall Conductivity in Ionospheric Heating Experiments

B. Tulegenov<sup>1</sup>  and A. V. Streltsov<sup>1</sup> 

<sup>1</sup>Department of Physical Sciences, Embry-Riddle Aeronautical University, Daytona Beach, FL, USA

**Abstract** We investigate the role of Hall conductivity in ionospheric heating experiments. Ionospheric heating by powerful X-mode waves changes the Hall and Pedersen conductances in the *E* and *D* regions, which lead to the generation of ultra-low frequency (ULF)/extremely-low frequency/very low frequency waves, when the electric field exists in the ionosphere. The importance of the Hall currents in the magnetosphere-ionosphere interactions, carried by ULF waves and field-aligned currents, has been consistently overlooked in studies devoted to the active experiments. Simulations of the three-dimensional two-fluid magnetohydrodynamic (MHD) model, presented in this paper, demonstrate that the Hall conductivity changes (1) the growth rate and the amplitude of ULF waves generated by the heating and (2) the orientation and the direction of propagation of the generated waves. These findings provide insight in the experiments where the waves were generated with a geometric modulation technique and suggest a new and more efficient approach for conducting such experiments in the future.

### 1. Introduction

Shear Alfvén waves carrying magnetic field-aligned currents (FACs) are one of the major participants in the redistribution of electromagnetic power, particle density, mass, and momentum between the ionosphere and magnetosphere at high latitudes (Chaston et al., 2002; Inan et al., 1985; Lysak, 1991; Streltsov & Lotko, 2008). That fact makes these waves an object of intensive experimental and theoretical study, and a large number of experiments devoted to the artificial excitation of these waves in the magnetosphere from the ground-based facilities have been conducted in Europe, Russia, and the United States for more than 60 years. Comprehensive reviews of these experiments and their results can be found in Gurevich (2007) and Streltsov et al. (2018).

One of the most well-known and widely used methods of generation of ultra-low frequency (ULF) waves from the ground is heating the ionosphere with X-mode high-frequency (HF) waves. These waves increase the bulk temperature of the electron population in the ionospheric *D* and *E* regions. The variations in the electron temperature change the Hall and Pedersen conductances in the ionosphere. Ionospheric conductivity is directly proportional to the ions' mobility. Studies and observations show that the ion mobility decreases by a factor of 1.4 or 2.0 when the ions are heated threefold or sevenfold by the perpendicular electric field, respectively (Aikio et al., 2004; Paschmann et al., 2003). If there is a large-scale electric field in the ionosphere, then the changes in the conductances cause changes in the Hall and Pedersen currents flowing in the ionosphere, which, in turn, generate magnetic FAC flowing into the magnetosphere. This is a so-called Getmantsev's effect (Getmantsev et al., 1974), which was introduced in 1974 and extensively used after that in the high-latitude ionosphere-magnetosphere system. The auroral and subauroral zones are particularly favorable for this mechanism because, normally, there is a large-scale electric field in the ionosphere associated with the electrojet (Gurevich, 1978; Robinson et al., 1998; Stubbe & Kopka, 1977; Stubbe et al., 1981).

If the frequency of the generated ULF waves matches one of the eigenfrequencies of the global magnetospheric resonator (formed by the entire magnetic flux tube and bounded by the ionosphere), then these waves can form a standing pattern along the magnetic field line between the conjugate hemispheres and reach large amplitudes after some time. Simulations by Streltsov et al. (2005, 2010) show that a large-amplitude (in the order of 50 nT) ULF wave can be generated even by a relatively small ionospheric disturbance modulated with the eigenfrequency of the resonator.

Because the HF power available for the ionospheric modification from ground transmitters is always limited, there are many theoretical and experimental studies devoted to the efficiency of how this power is used (Streltsov et al., 2018). Two of the most efficient methods described in the literature include “beam painting” and geometric modulation techniques. The beam painting technique, suggested by Papadopoulos et al. (1989, 1990), means that the beam focuses in a small spot, which moves rapidly across some area in the ionosphere to heat electrons inside this area. The entire process is modulated with the frequency of the generated wave. The geometric modulation means that instead of heating one spot (or some area) in the ionosphere and turning the transmitter ON and OFF with the wave period, the transmitter sends a constant beam of HF power and moves it in the ionosphere along some particular geometrical path. The injection of extremely-low frequency (ELF)/very-low frequency (VLF) waves into the magnetosphere by the modulated heating of the electrojet by the High Altitude Active Research Program (HAARP) facility in Alaska has been extensively studied by Papadopoulos et al. (2003), Golkowski et al. (2008, 2011), and Cohen et al. (2010).

Streltsov and Pedersen (2010) proposed a modification to the geometric modulation technique. They suggest to move the heating spot in the ionosphere in the direction of the background electric field with the phase speed of the feedback-unstable ULF wave. This suggestion was based on numerical simulations of the two-fluid magnetohydrodynamic (MHD) model describing active ionospheric response (also known as feedback) on the structure and amplitude of magnetospheric FACs interacting with the ionosphere and modifying conductivity by precipitating electrons in it. The ionospheric feedback mechanism has been studied for almost 50 years (Atkinson, 1970). The basic idea is that the ULF FAC changes the ionospheric conductivity (almost four-fold from 2.0 mho to less than 0.5 mho) by precipitating/removing electrons into/from the *E* layer and the variation in the conductivity “feedback” on the structure and amplitude of the incident FAC. When the large-scale electric field exists in the ionosphere, the feedback may work in a constructive way and increase the amplitude of the ULF waves and the density disturbances on the ionosphere, which lead to instability.

Streltsov and Pedersen (2010) used the X-mode heating to trigger and enhance the ionospheric feedback instability by synchronizing the heating regime with the dynamics of the most feedback-unstable ULF mode. This idea had been implemented during the 2014 BRIOCHE research campaign at HAARP and did not produce any positive results. There are several possible reasons why these particular experiments were not successful. Among them could be the absence of the electrojet, the high density of the ionosphere above the HAARP, unknown information about ionospheric parameters in the magnetically conjugate location, and so forth. However, there is one particular shortage in the Streltsov and Pedersen (2010) model, which may significantly compromise the applicability of the numerical results to real experiments. This shortage comes from the fact that the numerical model used was two-dimensional (with a one-dimensional ionosphere) and did not include effects of the Hall current in the ionosphere. At the same time, the importance of the Hall current for the ionospheric feedback mechanism has been emphasized in almost every classical paper about the instability (e.g., Atkinson, 1970; Borisov & Stubbe, 1997; Miura et al., 1982; Pokhotelov et al., 2000; Sato, 1978; Trakhtengerts & Feldstein, 1991).

The goal of this paper is to eliminate this shortage and investigate the effects of the Hall current on the dynamics of the magnetosphere-ionosphere interactions involving the ionospheric feedback mechanism triggered and controlled by the artificial ionospheric heating. This study is based on a 3-D reduced two-fluid MHD model described in the following sections.

## 2. Model and Numerical Implementation

The model used in this study is described in detail in Jia and Streltsov (2014). It consists of two coupled parts. The “magnetospheric” part describes propagation of the dispersive Alfvén waves and magnetic FACs in the magnetosphere, and the “ionospheric” part describes generation of the FACs by the perpendicular electric field and the ionospheric density disturbances caused by the heating. The ionospheric part also describes active feedback interactions between the magnetospheric FACs and the ionospheric density changes caused by these currents.

The magnetospheric part of the model includes the electron parallel momentum equation

$$\frac{\partial v_{\parallel e}}{\partial t} + v_{\parallel e} \nabla_{\parallel} v_{\parallel e} + \frac{e}{m_e} E_{\parallel} + \frac{1}{m_e n_0} \nabla_{\parallel} (n T_e) = -f_e v_{\parallel e}, \quad (1)$$

the current continuity equation

$$\nabla \cdot \left[ \left( \frac{1}{v_A^2} + \frac{1}{c^2} \right) \frac{\partial \mathbf{E}_\perp}{\partial t} \right] = \mu_0 \nabla \cdot (j_\parallel \mathbf{b}), \quad (2)$$

and the density continuity equation

$$\frac{\partial n}{\partial t} = -\nabla \cdot (n v_{\parallel e} \mathbf{b}). \quad (3)$$

Here subscripts  $\parallel$  and  $\perp$  indicate parallel and perpendicular vector components to  $\mathbf{b} = B_0/B_0$ , respectively,  $v_e$  is the electron velocity,  $n_0$  is the background quasi-neutral plasma density,  $T_e$  is the background electron temperature,  $f_e$  is the electron collision frequency,  $v_A = B_0/(\mu_0 n_0 m_i)^{0.5}$  is the Alfvén speed, and  $m_i$  is the proton mass. The collisional resistivity is included in the model because some studies (e.g., Borovsky, 1993; Lessard & Knudsen, 2001) suggest that it may cause an absorption of very small scale ( $\leq 1$  km) waves at altitudes below 1,000 km. The electron temperature is modeled as  $T_e = (T_{e^*} n_*)/n_0$ , where  $T_{e^*} = 2$  eV and  $n_*$  is the density at the equator. Such an assumption satisfies the equilibrium condition  $\nabla_z(n_0 T_e) = 0$ .

The ionospheric part consists of the density continuity equation

$$\frac{\partial n}{\partial t} = \frac{j_\parallel}{eh} + \alpha (n_0^2 - (1-H)n^2) \quad (4)$$

and the height-integrated current continuity equation

$$\nabla \cdot (\Sigma_P \mathbf{E}_\perp + \Sigma_H \mathbf{E}_\perp \times \mathbf{b}) = \pm j_\parallel. \quad (5)$$

Here,  $\Sigma_P = M_P n h e / \cos \lambda$  and  $\Sigma_H = M_H n h e / \cos \lambda$  are the height-integrated Pedersen and Hall conductivities;  $H$  indicates the effect of the HF heating on the recombination rate,  $M_P = 10^4$  m<sup>2</sup>/sV is the ion Pederson mobility, and  $M_H$  is the Hall mobility, which is one of the model's free parameters;  $h = 20$  km is the effective thickness of the  $E$  region;  $\lambda$  is the angle between the normal to the ionosphere and the corresponding dipole magnetic field line at 100-km altitude, and  $\alpha = 3 \times 10^7$  cm<sup>3</sup>/s is the recombination coefficient. The sign “+” in (5) is used in the Southern Hemisphere, and the sign “−” is used in the Northern Hemisphere.

Effect of the HF heating is modeled via a decrease in the coefficient of the recombination in the  $E$  region. It is specified by the function  $H(\rho)$  in (4), which is chosen as  $H(\rho) = 0.1 e^{-(\rho/\rho_0)^2}$ . Here  $\rho$  is the distance in the ionosphere from the center of the heated spot (where the heater power maximizes), and  $\rho_0 = 10$  km is a half width of the heated spot beam. The maximum amplitude of  $H$  at  $\rho = 0$  is 0.1, which means that the heating changes the coefficient of the recombination by 10%.

The model equations are written in the orthogonal dipole coordinates  $(L, \phi, \mu)$ , where  $L = r/\sin^2 \theta$ ,  $\mu = \cos \theta/r^2$ , and  $r, \theta$ , and  $\phi$  are spherical coordinates. Computations have been performed in the three-dimensional dipole magnetic flux tube bounded by the ionosphere in the Northern and Southern Hemispheres. The latitudinal boundaries of the domain are formed by the  $L = 4.6$  and  $L = 5.2$  magnetic shells. The azimuthal size of the domain is  $\phi = 1.91^\circ$ . The computational grid inside the domain has 101 steps in the  $L$  direction, 64 steps in the  $\phi$  direction, and 101 steps in the  $\mu$  direction. The steps are uniform in the  $L$  and  $\phi$  directions and strongly nonuniform in the  $\mu$  direction. In particular, the size of steps in the  $\mu$  direction decreases 200 times from the equator to the ionosphere, and as a result, the grid is denser at low altitudes and sparser in the equatorial magnetosphere. Periodic boundary conditions are implemented on the boundaries in the  $\phi$  direction, and the Dirichlet boundary conditions are implemented on the boundaries in the  $L$  direction.

### 2.1. Background Parameters

The background parameters of the model are similar to the typical parameters of the ionosphere-magnetosphere system considered in other studies (e.g., Streltsov & Pedersen, 2010). The geomagnetic field is assumed to be dipole,  $B_0 = B_* (1 + 3 \sin^2 \theta)^{0.5} / r^3$ , where  $B_* = 31,000$  nT and  $r$  is a geocentric distance in  $R_E = 6,371.2$  km.

The background density along the  $L = 4.9$  magnetic field line, whose ionospheric footprint corresponds to the HAARP location, is defined as

$$n_0 = \begin{cases} a_1(r - r_1) + a_2, & \text{if } r_1 < r < r_2 \\ b_1 e^{-20(r-r_2)} + b_2 r^{-4} + b_3, & \text{if } r > r_2. \end{cases} \quad (6)$$

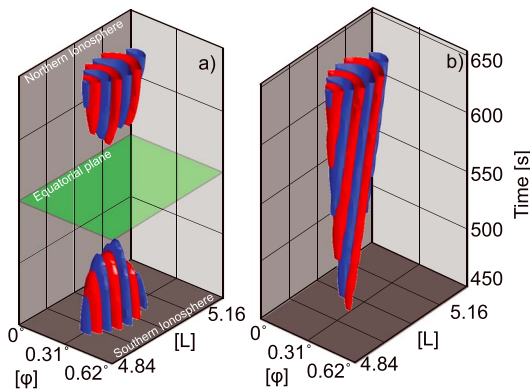


**Figure 1.** Isosurfaces of  $j_{\parallel} = -0.1 \mu\text{A}/\text{m}^2$  (blue) and  $j_{\parallel} = 0.1 \mu\text{A}/\text{m}^2$  (red) are shown from the 3-D magnetohydrodynamic simulation with  $\Sigma_H/\Sigma_P = 0$ . (a) The snapshot of the parallel current density,  $j_{\parallel}$ , generated by heating the Northern ionosphere at a fixed location at  $t = 651$  s. (b) Time evolution of  $j_{\parallel}$  on the Northern ionosphere generated by heating the Northern ionosphere at a fixed location.

Here  $r$  is the radial distance to point on the field line,  $r_1 = 1 + 100/R_e$  and  $r_2 = 1 + 220/R_e$ . The constants  $a_1$ ,  $a_2$ ,  $b_1$ ,  $b_2$ , and  $b_3$  are parameters that satisfy a density of  $1.00 \times 10^4 \text{ cm}^{-3}$  at  $E$  region altitude of 100 km,  $2.63 \times 10^5 \text{ cm}^{-3}$  at  $F$  region altitude of 220 km, and  $129 \text{ cm}^{-3}$  in the equatorial magnetosphere. The density of  $1.00 \times 10^4 \text{ cm}^{-3}$  in the  $E$  region provides the height-integrated Pedersen conductivity of 0.32 mho. Inside the computational domain, the density is assumed to be homogeneous in the direction perpendicular to the ambient magnetic field. This is a reasonable assumption due to the relatively small perpendicular size of the domain ( $0.6 L$  shell in the  $L$  direction and less than  $2^\circ$  in the  $\phi$  direction).

The background electric field in the domain is defined as  $E_0 = -\nabla\Phi$ , where  $\Phi$  is the electric potential. In the ionosphere, the potential  $\Phi$  is chosen to provide a uniform electric field with a magnitude 20 mV/m pointed in the north-south direction. This electric potential remains constant along the ambient magnetic field lines, so there is not any background parallel electric field (or the parallel potential drop) present in the magnetosphere. This field is comparable with the background electric field considered in 2-D simulations of the ionospheric heating by Streltsov and Pedersen (2010).

### 3. Results and Discussion

We start this section with a verification of the main results from the 2-D simulations by Streltsov and Pedersen (2010). Namely, that the movement of the heating spot in the ionosphere with the phase velocity of the feedback-unstable mode leads to a generation of larger amplitude waves in a shorter time than the heating of some stationary location in the ionosphere. To verify this result, we run the 3-D code with  $\Sigma_H = 0$ .

In the first run, the heating was focused on a stationary spot in the ionosphere. The results from this run are shown in Figure 1. In particular, Figure 1a shows a snapshot of the parallel current density  $j_{\parallel}$ , inside the 3-D domain, at time  $t = 651$  s after the beginning of heating.

Figure 1a shows the surfaces of  $j_{\parallel} = 0.1 \mu\text{A}/\text{m}^2$  in red and surfaces of  $j_{\parallel} = -0.1 \mu\text{A}/\text{m}^2$  in blue. Figure 1b shows the temporal dynamics of  $j_{\parallel}$  measured at an altitude of 100 km in the Northern Hemisphere. Again, the red color is used to show the surfaces of  $j_{\parallel} = 0.1 \mu\text{A}/\text{m}^2$  and the blue color is used to show the surfaces of  $j_{\parallel} = -0.1 \mu\text{A}/\text{m}^2$ . Figure 1 illustrates development of the ionospheric feedback instability driven by the uniform 20-mV/m electric field and triggered by the constant heating of the ionosphere.

The results from this run had been used to estimate the phase velocity of the feedback-unstable waves in the ionosphere. Comparison of  $j_{\parallel}$  in the ionosphere in several instances in time shows that the waves generated by the instability propagate in the direction of the background electric field (in this case it is the  $L$  direction) with a phase speed of  $\approx 100$  m/s. This value is equal to the phase velocity calculated from the linear dispersion relation given for the most unstable mode by Sato (1978), which for the parameters used in this study is  $\omega/k_{\perp} = M_P E_{10}/2 = 100$  m/s.

To model the moving of the heating spot in the ionosphere, we make the  $H$  function in equation (4) depending on time, namely,  $H = H(v_L t + L_0, v_{\phi} t + \phi_0)$ , where  $v_L$  and  $v_{\phi}$  are the wave front's phase velocity components estimated from the simulation with stationary heating spot in the ionosphere. In case  $\Sigma_H = 0$ , the  $L$  component of the phase velocity in the ionosphere is 100 m/s and  $v_{\phi} = 0$ . Figure 2 illustrates a comparison between  $j_{\parallel}$  obtained in the simulations with a stationary heating spot (left panels) and with a moving heating spot (right panels). In particular, Figures 2c and 2d show time evolution of  $j_{\parallel}$ , in the Northern Hemisphere ionosphere, at a 2-D longitudinal cut through the computational domain

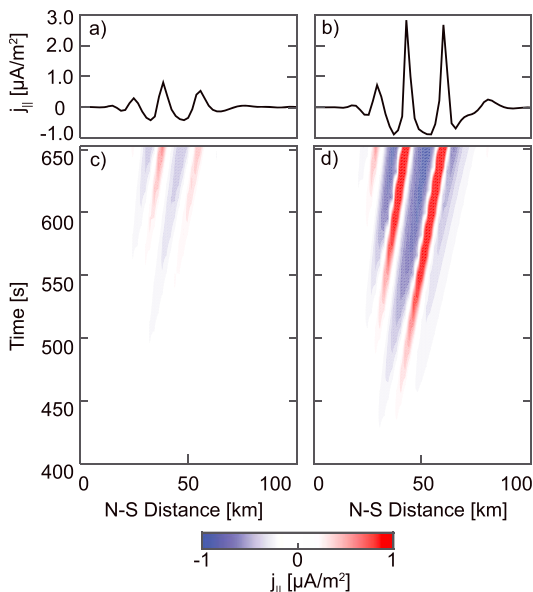


**Figure 2.** (a, c) The simulation output where the heater was heating a fixed location in the Northern ionosphere. (b, d) The simulation output in a case where the heating spot was moving in the direction of background  $E_{\perp}$  with velocity of 100 m/s. Panels (c) and (d) show the time evolution of field-aligned currents on the Northern ionosphere along the direction of background electric field from  $L = 4.84$  to  $L = 5.16$  in a case when  $\Sigma_H/\Sigma_P = 0$ . Panels (a) and (b) show the amplitude of the field-aligned currents at  $t = 651$  s.

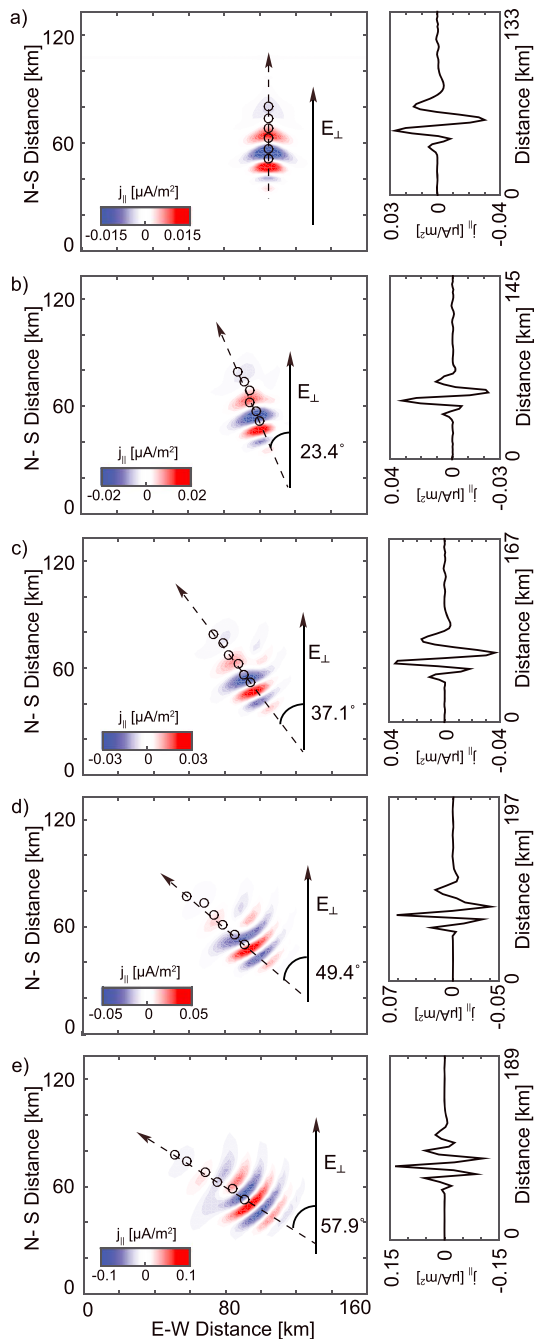


**Figure 3.** Snapshots of  $j_{\parallel}$  on the Northern ionosphere at  $t = 356$  s under different ionospheric conditions: (a)  $\Sigma_H/\Sigma_P = 0$ , (b)  $\Sigma_H/\Sigma_P = 0.5$ , (c)  $\Sigma_H/\Sigma_P = 1.0$ , (d)  $\Sigma_H/\Sigma_P = 1.5$ , and (e)  $\Sigma_H/\Sigma_P = 2.0$ . The line plots in each panel show the amplitude of field-aligned current along the dashed arrow. The black circles indicate the propagation in time of the first wave fronts. The time step between circles is 59.43 s.

at  $L = 4.9$  from  $t = 400$  s to  $t = 651$  s after the heater was turned on. Figures 2a and 2b show magnitudes of  $j_{\parallel}$  in the ionosphere in the Northern Hemisphere at  $t = 651$  s.

Figure 2 demonstrates that the ULF waves are generated faster when the heater moves along the  $E_{\perp}$ . The amplitudes of the waves generated by moving the heating spot are  $\approx 3$  times larger than those generated by heating a fixed spot in the ionosphere. These results confirm the conclusion made by Streltsov and Pedersen (2010) that without Hall current in the ionosphere the instability indeed develops more rapidly when the heating spot moves along the direction of the background electric field at the phase velocity of the wave front.

Next, we perform 3-D simulation of the instability initiated by the heating of a stationary spot in the ionosphere when the Hall conductivity is not equal to zero. Figure 3 shows the structure and magnitude of  $j_{\parallel}$  in the Northern Hemisphere ionosphere at time  $t = 356$  s in simulations with  $\Sigma_P = 0.32$  mho and (a)  $\Sigma_H/\Sigma_P = 0$ , (b)  $\Sigma_H/\Sigma_P = 0.5$ , (c)  $\Sigma_H/\Sigma_P = 1.0$ , (d)  $\Sigma_H/\Sigma_P = 1.5$ , and (e)  $\Sigma_H/\Sigma_P = 2.0$ . It shows two effects. First, the amplitude of  $j_{\parallel}$  increases with the increase of  $\Sigma_H$ . This effect follows directly from equation (5), which shows that the magnitude of  $j_{\parallel}$  in the ionosphere is proportional to  $\Sigma_P$ ,  $\Sigma_H$ , and  $E_{\perp}$ ; therefore, if one of these three parameters increases and two other remain constant, then  $j_{\parallel}$  is expected to increase as well.

The second effect shown in Figure 3 is that the feedback-unstable waves propagate across the magnetic field in the direction that makes an angle with the background  $E_{\perp}$  (which is in the north-south direction in all these simulations). This angle increases with an increase in  $\Sigma_H/\Sigma_P$ . This effect is also expected, and it has been previously reported by Jia and Streltsov (2014) from the simulations of discrete auroral arcs produced by the ionospheric feedback mechanism involving the Hall conductivity. This can be explained by the fact that in the magnetosphere-ionosphere coupled system, the magnetic FACs are closed in the ionosphere by Hall and Pedersen currents. Therefore, larger Hall conductivity provides a greater contribution from the Hall current, and the entire current system changes its orientation with increase in  $\Sigma_H/\Sigma_P$ .

The angles between the wave phase velocity and the background electric field observed in the simulations for different values of  $\Sigma_H/\Sigma_P$  are  $0^{\circ}$ ,  $23.4^{\circ}$ ,  $37.1^{\circ}$ ,  $49.4^{\circ}$ , and  $57.9^{\circ}$ . The corresponding angles calculated analytically as  $\arctan(\Sigma_H/\Sigma_P)$  are  $0^{\circ}$ ,  $26.6^{\circ}$ ,  $45.0^{\circ}$ ,  $56.3^{\circ}$ , and  $63.4^{\circ}$ . The analytical and numerical sets of angles show the same dependency on the  $\Sigma_H/\Sigma_P$  ratio, but they are different in magnitudes. The possible explanation of the differences between the corresponding values is that the angle calculated as  $\arctan(\Sigma_H/\Sigma_P)$  assumes that the electric field is constant. This assumption does not work when the amplitude of the feedback-unstable waves reaches larger value. At this stage, the amplitude of the electric field produced in the ionosphere by the waves becomes comparable with the amplitude of the background field: so the amplitude and the orientation of the total field in the ionosphere differ from the background/initial field.

To evaluate the effect of the moving heating spot on the development of the instability, a simulation was performed with the heating spot moving in the ionosphere with a velocity estimated from the simulations with stationary heating. Thus, the circles in Figure 3 indicate locations of the first wavelength of the generated wave in time. Figure 4 shows  $j_{\parallel}$  in the Northern ionosphere obtained from the simulations with  $\Sigma_H/\Sigma_P = 2.0$  at time  $t = 356$  s (a) when the heating spot is fixed in space and (b) when the heating spot moves at the angle

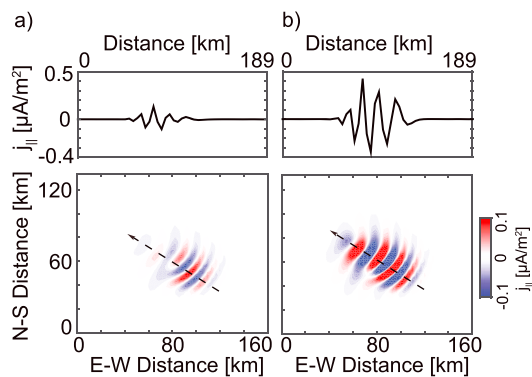


**Figure 4.** The snapshots of the  $j_{\parallel}$  at  $t = 356$  s on the Northern ionosphere from simulations with  $\Sigma_H/\Sigma_P = 2.0$  under different heating methods: (a) fixed heating spot and (b) moving heating spot. The line plots in both panels show the amplitude of field-aligned current along the dashed arrow.

of  $57.9^\circ$  to the background  $E_{\perp}$  with a velocity  $v_L = 133$  m/s and  $v_{\phi} = 83.4$  m/s, which correspond to the phase velocity of the first wave front. Figure 4 demonstrates that similar to the case with no Hall current, the ULF waves are generated more efficiently (they reach larger amplitude faster), when the ionospheric feedback mechanism is “enhanced” by the moving heating spot in the ionosphere with the wave phase velocity.

This finding may provide a possible explanation of the failure of the experiments with the “directional” heating described in this study in the 2014 BRIOCHE HAARP campaign: These experiments were based on 2-D simulations not taking into account the Hall current in the ionosphere. The effect of this current is quite significant, particularly, when  $\Sigma_H/\Sigma_P = 2.0$ . It may also explain the more efficient wave generation observed in some experiments with the geometric modulation of heating reported by Cohen et al. (2008, 2010). Our results suggest that the heating is more efficient when the heating spot moves with a velocity which component in the direction of the total ionospheric current is close to the phase velocity of the feedback-unstable waves. Possibly, such an agree-

ment between the velocity of the heating spot and the phase speed of the generated waves happened during some of experiments with geometric modulation of the ionosphere.

There are two major conclusions from our study. The first one is that the Hall conductivity indeed plays an important role in the generation of large-amplitude ULF waves by the ionospheric feedback mechanism driven by the electric field in the ionosphere. Our simulations confirm results from earlier studies that the Hall conductivity (1) increases the growth rate of the instability and (2) changes the direction of propagation of the feedback-unstable waves relative to the background electric field in the ionosphere. The second conclusion is that the efficiency of generation of ULF waves by the ionospheric HF heating can be increased significantly by moving the heating spot with a phase velocity of the feedback-unstable waves taking into account the presence of the Hall current in the ionosphere. The amplitude and direction of this velocity can be estimated during the experiment from the observations of plasma density, temperature, and the ion drift speed with phase radars (if they are available) and digisonds and from 3-D numerical simulations performed in advance for various possible combinations of the background parameters.

#### Acknowledgments

The authors would like to acknowledge the support of ERAU’s Department of Physical Sciences in publishing this article. The executable code, the input parameters, and the numerical results shown in Figures 1–4 are available on Figshare.com (<https://doi.org/10.6084/m9.figshare.7994306>).

#### References

- Aikio, A. T., Mursula, K., Buchert, S., Forme, F., Amm, O., Marklund, G., et al. (2004). Temporal evolution of two auroral arcs as measured by the cluster satellite and coordinated ground-based instruments. *Annales Geophysicae*, 22, 4089–4101. <https://doi.org/10.5194/angeo-22-4089-2004>
- Atkinson, G. (1970). Auroral arcs: Result of the interaction of a dynamic magnetosphere with the ionosphere. *Journal of Geophysical Research*, 75, 4746–4755. <https://doi.org/10.1029/JA075i025p04746>
- Borisov, N., & Stubbe, P. (1997). Excitation of longitudinal (field-aligned) currents by modulated HF heating of the ionosphere. *Journal of Atmospheric and Solar-Terrestrial Physics*, 59, 1973–1989. [https://doi.org/10.1016/S1364-6826\(97\)00019-9](https://doi.org/10.1016/S1364-6826(97)00019-9)
- Borovsky, J. E. (1993). Auroral arc thicknesses as predicted by various theories. *Journal of Geophysical Research*, 75, 4746–4755. <https://doi.org/10.1029/92JA02242>
- Chaston, C. C., Bonnell, J. W., Carlson, C. W., Berthomier, M., Peticolas, L. M., Roth, I., et al. (2002). Electron acceleration in the ionospheric Alfvén resonator. *Journal of Geophysical Research*, 107(A11), 1413. <https://doi.org/10.1029/2002JA009272>
- Cohen, M. B., Inan, U. S., & Golkowski, M. A. (2008). Geometric modulation: A more effective method of steerable ELF/VLF wave generation with continuous HF heating of the lower ionosphere. *Geophysical Research Letters*, 35, L12101. <https://doi.org/10.1029/2008GL034061>
- Cohen, M. B., Inan, U. S., Golkowski, M. A., & McCarrick, M. J. (2010). ELF/VLF wave generation via ionospheric HF heating: Experimental comparison of amplitude modulation, beam painting, and geometric modulation. *Journal of Geophysical Research*, 115, A02302. <https://doi.org/10.1029/2009JA014410>
- Getmantsev, G., Zuikov, N., Kotik, D., Mironenko, L., Mityakov, N., Rapoport, V., et al. (1974). Combination frequencies in the interaction between high-power short-wave radiation and ionospheric plasma. *ZhETF Pis’ma Red.*, 20, 101.
- Golkowski, M., Cohen, M. B., Carpenter, D. L., & Inan, U. S. (2011). On the occurrence of ground observations of ELF/VLF magnetospheric amplification induced by the HAARP facility. *Journal of Geophysical Research*, 116, A04208. <https://doi.org/10.1029/2010JA016261>
- Golkowski, M., Inan, U. S., Gibby, A. R., & Cohen, M. B. (2008). Magnetospheric amplification and emission triggering by ELF/VLF waves injected by the 3.6 MW HAARP ionospheric heater. *Journal of Geophysical Research*, 113, A10201. <https://doi.org/10.1029/2008JA013157>
- Gurevich, A. (1978). *Nonlinear phenomena in the ionosphere*. New York: Springer-Verlag.
- Gurevich, A. (2007). Nonlinear effects in the ionosphere. *Phys.-Uspekhi*, 50(11), 1091. <https://doi.org/10.1070/PU2007v050n11ABEH006212>

- Inan, U. S., Chang, H. C., Helliwell, R. A., Imhof, W. L., Reagan, J. B., & Walt, M. (1985). Precipitation of radiation belt electrons by man-made waves: A comparison between theory and measurement. *Journal of Geophysical Research*, *90*(A1), 359–369. <https://doi.org/10.1029/JA090iA01p00359>
- Jia, N., & Streltsov, A. V. (2014). Ionospheric feedback instability and active discrete auroral forms. *Journal of Geophysical Research: Space Physics*, *119*, 2243–2254. <https://doi.org/10.1002/2013JA019217>
- Lessard, M. R., & Knudsen, D. J. (2001). Ionospheric reflection of small-scale Alfvén waves. *Geophysical Research Letters*, *28*, 3573–3576. <https://doi.org/10.1029/2000GL012529>
- Lysak, R. L. (1991). Feedback instability of the ionospheric resonant cavity. *Journal of Geophysical Research*, *96*(A2), 1553–1568. <https://doi.org/10.1029/90JA02154>
- Miura, A., Ohtsuka, S., & Tamao, T. (1982). Coupling instability of the shear Alfvén wave in the magnetosphere with the ionospheric ion drift wave. 2. Numerical analysis. *Journal of Geophysical Research*, *87*(A2), 843–851. <https://doi.org/10.1029/JA087iA02p00843>
- Papadopoulos, K., Chang, C. L., Vitello, P., & Drobot, A. (1990). On the efficiency of ionospheric ELF generation. *Radio Science*, *25*(6), 1311–1320. <https://doi.org/10.1029/RS025i006p01311>
- Papadopoulos, K., Sharma, A. S., & Chang, C. L. (1989). On the efficient operation of a plasma ELF antenna driven by modulation of ionospheric currents. *Comments Plasma Physics Controlled Fusion*, *13*(1), 1–17.
- Papadopoulos, K., Wallace, T., McCarrick, M., Milikh, G. M., & Yang, X. (2003). On the efficiency of ELF/VLF generation using HF heating of the auroral electrojet. *Plasma Physics Reports*, *29*, 561. <https://doi.org/10.1134/1.1592554>
- Paschmann, G., Haaland, S., & Treumann, R. (Eds.) (2003). *Auroral plasma physics*, *J. Geophys. Res. Edited by Paschmann, G., Haaland, S., & Treumann, R.* Netherlands: Springer Netherlands.
- Pokhotelov, O. A., Pokhotelov, D., Streltsov, A., Khrushev, V., & Parrot, M. (2000). Dispersive ionospheric Alfvén resonator. *Journal of Geophysical Research*, *105*(A4), 7737–7746. <https://doi.org/10.1029/1999JA900480>
- Robinson, T. R., Bond, G., Eglitis, P., Honary, F., & Rietveld, M. T. (1998). RF heating in a strong auroral electrojet. *Advances in Space Research*, *21*(5), 689–692. [https://doi.org/10.1016/S0273-1177\(97\)01004-1](https://doi.org/10.1016/S0273-1177(97)01004-1)
- Sato, T. (1978). A theory of quiet auroral arcs. *Journal of Geophysical Research*, *83*(A3), 1042–1048. <https://doi.org/10.1029/JA083iA03p01042>
- Streltsov, A. V., Berthelier, J.-J., Chernyshov, A. A., Frolov, L. V., Honary, F., Kosch, M. J., et al. (2018). Past, present and future of active radio frequency experiments in space. *Space Science Reviews*, *214*, 122. <https://doi.org/10.1007/s11214-018-0549-7>
- Streltsov, A. V., & Lotko, W. (2008). Coupling between density structures, electromagnetic waves and ionospheric feedback in the auroral zone. *Journal of Geophysical Research*, *113*, A05212. <https://doi.org/10.1029/2007JA012594>
- Streltsov, A., Lotko, W., & Milikh, G. (2005). Simulations of ULF field-aligned currents generated by HF heating of the ionosphere. *Journal of Geophysical Research*, *110*, 629. <https://doi.org/10.1029/2004JA010>
- Streltsov, A. V., & Pedersen, T. R. (2010). An alternative method for generation of ULF waves by ionospheric heating. *Geophysical Research Letters*, *37*, L14101. <https://doi.org/10.1029/2010GL043543>
- Streltsov, A. V., Pedersen, T. R., Mishin, E. V., & Snyder, A. L. (2010). Ionospheric feedback instability and substorm development. *Journal of Geophysical Research*, *115*, A07205. <https://doi.org/10.1029/2009JA014961>
- Stubbe, P., & Kopka, H. (1977). Modulation of the polar electrojet by powerful HF waves. *Journal of Geophysical Research*, *82*(16), 2319–2325. <https://doi.org/10.1029/JA082i016p02319>
- Stubbe, P., Kopka, H., & Dowden, R. L. (1981). Generation of ELF and VLF waves by polar electrojet modulation: Experimental results. *Journal of Geophysical Research*, *86*(A11), 9073. <https://doi.org/10.1029/JA086iA11p09073>
- Trakhtengerts, V. Y., & Feldstein, A. Y. (1991). Turbulent Alfvén boundary layer in the polar ionosphere: 1. Excitation conditions and energetics. *Journal of Geophysical Research*, *96*(A11), 19,363–19,374. <https://doi.org/10.1029/91JA00376>